# Reset of human neocortical oscillations during a working memory task

D. S. Rizzuto*†, J. R. Madsen‡§, E. B. Bromfield¶, A. Schulze-Bonhage‖, D. Seelig*, R. Aschenbrenner-Scheibe‖, and M. J. Kahana*‡**

*Volen Center for Complex Systems, Brandeis University, Waltham, MA 02454; ‡Department of Neurosurgery, Children's Hospital, Boston, MA 02115; §Department of Surgery, Harvard Medical School, Boston, MA 02115; ¶Department of Neurology, Brigham and Women's Hospital, Boston, MA 02115; and ‖Neurozentrum, Universitaet Freiburg, D-79106 Freiburg, Germany

Communicated by Saul Sternberg, University of Pennsylvania, Philadelphia, PA, April 8, 2003 (received for review May 22, 2002)

**Both amplitude and phase of rhythmic slow-wave electroencephalographic activity are physiological correlates of learning and memory in rodents. In humans, oscillatory amplitude has been shown to correlate with memory; however, the role of oscillatory phase in human memory is unknown. We recorded intracranial electroencephalogram from human cortical and hippocampal areas while subjects performed a short-term recognition memory task. On each trial, a series of four list items was presented followed by a memory probe. We found agreement across trials of the phase of oscillations in the 7- to 16-Hz range after randomly timed stimulus events, evidence that these events either caused a phase shift in the underlying oscillation or initiated a new oscillation. Phase locking in this frequency range was not generally associated with increased poststimulus power, suggesting that stimulus events reset the phase of ongoing oscillations. Different stimulus classes selectively modulated this phase reset effect, with topographically distinct sets of recording sites exhibiting preferential reset to either probe items or to list items. These findings implicate the reset of brain oscillations in human working memory.**

Human brain oscillations are correlates of a diverse range of functions, including spatial learning (1), visual memory maintenance (2), verbal memory encoding (3), and sensory integration (see ref. 4 for a review). Although brain oscillations have long been studied using scalp-recorded electroencephalographic (EEG) signals, recent studies using intracranial EEG (iEEG) recordings overcome the poor spatial resolution inherent in scalp EEG (5). iEEG recordings can be ethically obtained in cases of medically resistive epilepsy, where they are clinically used to precisely localize regions of seizure onset. Because iEEG can measure activity from much smaller volumes than scalp EEG (6, 7), it can detect signals that change rapidly across the cortical surface and might otherwise remain undetected at the scalp due to spatial averaging. Furthermore, intracranial electrodes, which are often arrayed over the ventral surface of the brain, or implanted in the hippocampus, provide direct access to brain activity within these deep brain structures (e.g., ref. 8).

A number of studies have used intracranial recordings to study human brain oscillations with high spatial and temporal resolution. These studies have found high-amplitude oscillations in the 4- to 12-Hz frequency band that correlate with a number of behavioral states, including maze learning and verbal working memory (1, 9, 10). The 4- to 12-Hz oscillations observed during maze learning, and often visible in the unfiltered iEEG record, appear very much like those seen in rodent hippocampus during spatial exploration (see refs. 11 and 12 for reviews). Some investigators have suggested that these oscillations may be specific to tasks involving a spatial component (13); however, the discovery of high-amplitude 8-Hz activity during verbal working memory tasks, both intracranially (10) and at the scalp (14), suggests that these oscillations may play a more general role in human cognition, possibly associated with general purpose learning and cognitive control mechanisms (5).

A possible link between oscillatory phase and learning comes from rodent studies of long-term potentiation (LTP). LTP is highly sensitive to the phase of hippocampal slow wave activity, with potentiation favored at the peak of the oscillation and depotentiation favored at its trough. This finding, which has been observed both *in vitro* (15) and *in vivo* (16), suggests that slow-wave oscillations act as a windowing mechanism for synaptic plasticity. If oscillatory phase is crucial for LTP, then one might expect that memory-related stimulus events would produce a reset or phase shift of the ongoing oscillation. Consistent with this hypothesis, Givens (17) found that 8-Hz hippocampal activity in rats exhibited phase locking to test stimuli requiring a comparison with other recently presented stimuli. Also, Buzsaki and colleagues (18) found that rodent hippocampal oscillations reset in response to the conditioned stimulus in a classical conditioning task, whereas Adey (19, 20) found that, in cats, oscillatory phase locking was associated with increased performance in a T-maze task.

By pointing to a key role for oscillatory phase in animal cognition, these findings led us to examine the role of oscillatory phase in human cognition. In particular, we hypothesized that task events requiring encoding or retrieval processing would reset the phase of ongoing oscillations. We tested this hypothesis by recording iEEG signals while patients performed a verbal working memory task (21). This task was chosen because it had reliably induced high amplitude cortical oscillations in a previous study (10).

## Methods

**Participants.** We tested nine subjects who had been surgically implanted with cortical surface (subdural) and/or bilateral depth electrodes. The clinical team determined the placement of these electrodes so as to best localize epileptogenic regions. We recorded from a total of 689 electrodes; 138 of these were either (*i*) in the epileptic focus, (*ii*) overlying regions of radiographically evident structural brain damage, or (*iii*) exhibited epileptiform EEG (i.e., spikes and/or sharp waves, as determined by the clinical team). We restricted our analyses to the remaining 551 electrodes. Fig. 6, which is published as supporting information on the PNAS web site, www.pnas.org, illustrates the positions of the electrodes. All subjects had normal range personality and intelligence and were able to perform the task within normal limits (see Table 2, which is published as supporting information on the PNAS web site). Our research protocol was approved by the institutional review boards at Children's Hospital (Boston), Brigham and Women's Hospital (Boston), and Universitaetsklinikum (Freiburg, Germany). Informed consent was obtained from the subjects and their guardians.

Abbreviations: EEG, electroencephalography; iEEG, intracranial EEG.

†Present address: Division of Biology, California Institute of Technology, Pasadena, CA 91125.

**To whom correspondence should be addressed. E-mail: kahana@brandeis.edu.

NEUROSCIENCE

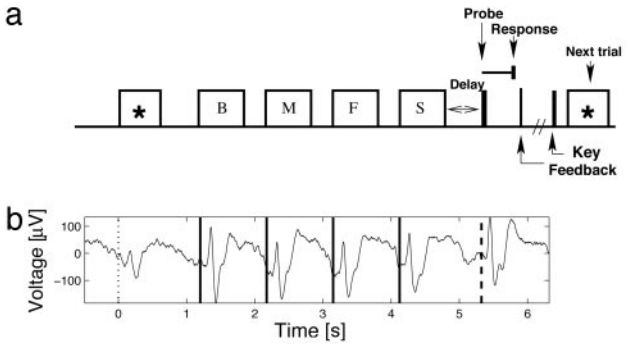


**Fig. 1.** The Sternberg item recognition task. (*a*) Illustration of the experimental design. (*b*) Average activity recorded from a representative electrode. Onset of the orienting stimulus is denoted by the dotted vertical line, the four list items by the solid lines and the probe is denoted by the dashed line. Electrode located in the left inferior temporal lobe of participant 5. [Talairach coordinates: (L–R, A–P, I–S) = (−33, −56, −17) mm.]

**Procedure.** Fig. 1*a* illustrates the behavioral task. The participant pressed a key on a computer keyboard to initiate each trial. An orienting stimulus (asterisk) was then displayed and remained visible for 1 s. All task stimuli appeared at the center of the computer screen. After a delay of 200 ± 75 ms (uniformly distributed), four consonants were sequentially displayed. The temporal jitter was introduced to ensure that each stimulus arrived at a random phase with respect to ongoing oscillations, so that prestimulus phase was uniformly distributed.[††] Each consonant was displayed for 700 ms followed by a delay of 275 ± 75 ms. List items and lures were randomly selected subject to the constraint that a particular consonant not repeat within three successive lists. The last (fourth) consonant was followed by a retention interval of 500 ± 75 ms and the presentation of the probe. The participant was instructed to indicate as quickly and accurately as possible whether the probe item either was in the preceding list (a target) or was not in the preceding list (a lure) by pressing the right-hand control key to target items and the left-hand control key to lures. Targets and lures occurred with equal probability, and target items were drawn equally from each of the list positions. Because there are few error trials during this task (<5%), we restrict our analyses to correct trials.

**iEEG Recordings.** The iEEG signal was recorded from platinum electrodes (3-mm diameter) with an inter-electrode spacing of 1 cm (for subdural electrodes) or 8 mm (for depth electrodes). The signal was amplified, sampled at 256 Hz (Children's Hospital, Bio-Logic apparatus: subjects 1–6; Universitaet Freiburg, Delta-Med SA apparatus: subject 7) or 200 Hz (Brigham and Women's Hospital, Nicolet Biomedical apparatus: subjects 8 and 9), and band-pass filtered (Bio-Logic, 0.3–70 Hz; DeltaMed SA, 0.015–120 Hz; Nicolet Biomedical, 0.5–60 Hz). For all subjects, the locations of the electrodes were determined by using coregistered postoperative computed tomography scans (CTs) and preoperative MRIs by an indirect stereotactic technique.

**Analysis of Phase Locking.** For each correct trial in the experiment, instantaneous phase was calculated for logarithmically spaced frequencies between 4 and 55 Hz ($2^{x/4}$ Hz, for $x \in 8, \ldots, 23$). Instantaneous phase was calculated by wavelet transforming the raw signal (using a 4-cycle Morlet wavelet) and calculating the angle of the resulting complex coefficients. For each frequency, the wavelet transformation of the intracranial signal produces a complex time series $w_{t,k}$, where $t$ represents the time point within trial $k$. Instantaneous phase, $\phi_{t,k} = \arctan(Im(w_{t,k})/Re(w_{t,k}))$.

The null hypothesis of uniformity for the distribution of $\phi_t$ (across $N$ correct trials) was tested using the Rayleigh statistic (22, 23),

$$\bar{R}_t = \frac{\sqrt{(\Sigma_{k=1}^{N} \cos \phi_{t,k})^2 + (\Sigma_{k=1}^{N} \sin \phi_{t,k})^2}}{N}. \quad [1]$$

An electrode was considered to exhibit phase locking at a given frequency if the phase distributions departed from uniformity (Rayleigh test, $P < 0.0001$) for all samples throughout a two-period interval during the 500 ms after stimulus onset. For example, a 10-Hz oscillation would have to exceed the $P$ value threshold for all samples within a 200-ms interval, whereas a 50-Hz oscillation would have to exceed the threshold for all samples within a 40-ms interval to meet this criterion.

We estimated the number of electrodes exhibiting phase locking separately for each stimulus class (orienting stimulus, list items, and probe) and used a bootstrap method to gauge the Type-I error in this estimate. To estimate the Type-I error at each frequency, the phase of iEEG activity within each trial was randomly shuffled across sampled time points and reanalyzed 100 times by using the same parameters, producing a distribution of the number of electrodes exhibiting phase locking for each stimulus class. For a given frequency to obtain significance, the true number of electrodes exhibiting phase locking must exceed the 99th percentile of this distribution ($P < 0.01$).

To assess the degree of phase locking to list items, the phase distributions were combined (after aligning the means) across serial positions 1–4. This was justified by the fact that although many electrodes exhibited phase locking to list items, there were no consistent differences in phase locking among the four serial positions. Thus, of the 551 electrodes, only two exhibited significant differences across serial positions in the 9- to 12-Hz range, and neither of these exhibited a consistent trend across serial position.

**Analysis of Preferential Reset.** Electrode were then tested for equality of concentration (24, 25) between stimulus classes. Pairwise comparisons were made only for those electrodes and frequencies that exhibited phase locking. The concentration of a circular distribution is analogous to the variance of a linear distribution, and this test directly compared the variance in phase locking across the orienting stimulus, list items, and the probe. Phase concentration, $d_i$, for each stimulus class $i$ was estimated using the circular sample mean, $\hat{\mu}_i$, as

$$d_i = \frac{1}{N} \sum_{j=1}^{N} |\sin \phi_{i,j} - \hat{\mu}_i| \quad [2]$$

and an $F$ ratio specific to circular distributions was used to compare concentrations across stimulus classes (25).

For all three pairwise comparisons among the three stimulus classes, we assessed differences at every sampled time point throughout the 500-ms interval after stimulus presentation for five different frequency bands (see Table 1). An electrode was deemed to exhibit preferential reset to a particular stimulus class in a given frequency band if its phase dispersion was consistently smaller ($P < 0.05$ for 0.5 cycles) than the dispersion of the other two stimulus classes for at least one frequency within the band,

[††]This amount of jitter (150 ms) will fully randomize prestimulus phase for all frequencies above 6.6 Hz. At 4 Hz, the lowest frequency we consider, this amount of jitter will ensure that prestimulus phase is, at a minimum, uniformly distributed within a 270° arc (of a possible 360°). Analyses take temporal jitter into account by selecting epochs of iEEG that have been aligned to the stimulus in question. Because of the inclusion of temporal jitter, a given stimulus had a slightly different onset from trial to trial. Therefore, figures that show average activity across the entire trial (Figs. 1*b* and 3) utilize epochs of stimulus-aligned iEEG after each stimulus onset, concatenating them to illustrate the full time course of the trial. These figures thus contain a discontinuity at the time of stimulus onset.

**Table 1. The precision of phase reset is modulated by task demands**

| Frequency band, Hz | Stimulus class | | |
|---|---|---|---|
| | Orienting | List items | Memory probes |
| 4–7 | 1 | 13* | 22* |
| 7–12 | 2* | 6* | 27* |
| 12–16 | 0 | 3* | 17* |
| 16–20 | 0 | 1* | 7* |
| 20–30 | 0 | 0 | 0 |
| 30–55 | 0 | 0 | 0 |

The number of electrodes exhibiting preferental reset to each stimulus class in each frequency band is shown. Asterisks denote an effect exceeding the estimated Type-I error rate ($P < 0.01$).

and if no other stimulus class obtained a significantly smaller phase dispersion at any frequency within the band.

As in our analysis of phase locking, we tallied the number of electrodes exhibiting preferential reset to each stimulus class using a bootstrap method to assess the Type-I error rate. The iEEG signal for each stimulus presentation was randomly assigned to a stimulus class and the classes were then reanalyzed for equality of concentration 100 times using the same thresholds, producing a distribution of the number of electrodes classified as exhibiting preferential reset. To obtain significance, the true number of electrodes exhibiting preferential reset must exceed the 99th percentile of this distribution ($P < 0.01$).

**Analysis of Postprobe Power.** To assess the contribution of evoked activity to phase locking, we correlated postprobe changes in wavelet power (the square of the norm of the wavelet-transformed signal) with postprobe phase locking across all electrodes. The measure of power change was the $t$ value from a paired-sample $t$ test comparing the log-transformed power in the 500-ms intervals before and after the onset of the probe. The measure of phase locking was the average value of the Rayleigh statistic for the 500-ms postprobe interval.

## Results

Participants performed the task with reasonably high accuracy (see Table 1) and with a mean reaction time (≈1 s) that was not much longer than one would expect under laboratory conditions (i.e., 550–750 ms; see refs. 21 and 26). As has been found in some previous studies (e.g., ref. 26), participants exhibited only modest serial position effects, having slightly faster responses when probed with the most recently presented item (data not shown).

In analyzing the electrophysiological data associated with this task, we first present results for selected electrodes that clearly illustrate some of the patterns present in these data. We follow these analyses with statistical tests aimed at summarizing the electrophysiological pattern across our entire data set.

Fig. 2*a* shows filtered iEEG traces from one electrode on four trials, recorded during the 1-s interval centered around probe onset, as well as the average of the filtered traces across all trials. Before the probes appearance (at time $t = 0$) oscillatory phase is seemingly random from trial to trial; that is, the peaks and troughs are not aligned. In contrast, after probe onset the peaks and troughs are aligned, accompanied by a large increase in the amplitude of the oscillation in the average trace.

The phase characteristics of oscillatory activity can be measured directly using spectral methods. The raw iEEG signal for each trial is first wavelet transformed, the phase angle calculated, and then the phase distribution (across trials) is examined. Fig. 2*b* shows the 8-Hz phase distribution taken 250 ms before the onset of the probe for the same electrode. This figure shows that the phase distribution is approximately uniform and exhibits no

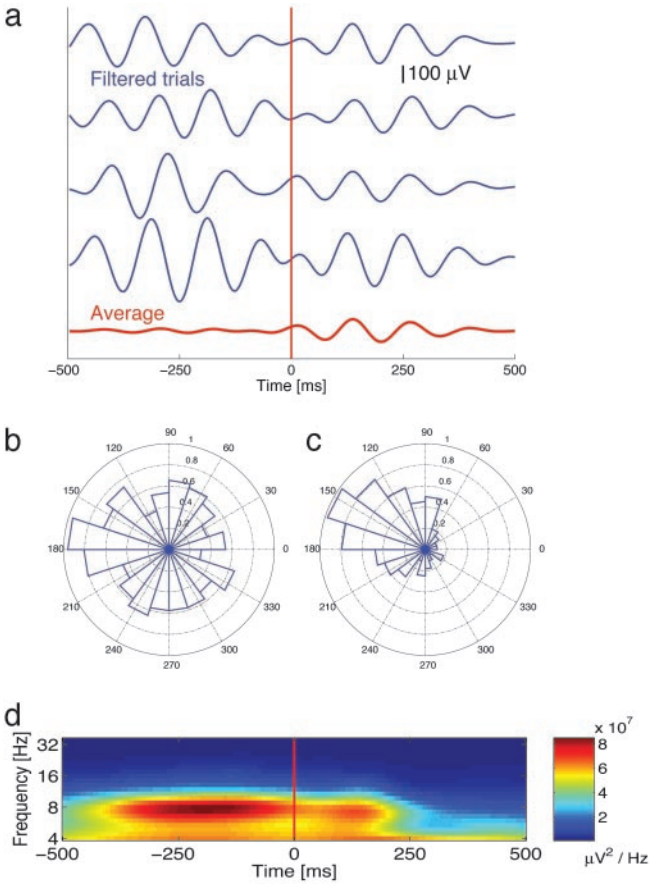


**Fig. 2.** Probes reset 8-Hz phase. (*a*) Filtered (6–10 Hz) single trials (blue lines) and average activity (red line) illustrating phase reset to the probes at the level of single trials for the 1-s interval surrounding probe onset (occuring at time $t = 0$). (*b*) An 8-Hz phase distribution 250 ms before the onset of the probe (calculated across 320 trials) is shown. (*c*) An 8-Hz phase distribution 250 ms after probe onset is shown. (*d*) Spectrogram showing average power (calculated across all trials, without filtering) at each frequency for the 1-s interval surrounding probe onset. For all panels, the electrode is the same as in Fig. 1*b*.

evidence of clustering. Indeed, we cannot reject the hypothesis that these phase data are drawn from a uniform distribution (Rayleigh test, $P > 0.5$). In comparison, Fig. 2*c* shows the 8-Hz phase distribution 250 ms after onset of the probe (the approximate time of maximal phase locking). This distribution exhibits significantly more phase clustering, and a Rayleigh test indicates that these data are not uniformly distributed ($P < 0.0001$).

The phase locking of single trial activity postprobe suggests that the phase of the oscillation is being reset due to the onset of the probe. However, it is possible that the observation of phase locking is instead an artifact of transient increases in power following probe presentation. For example, if the onset of the probe evoked an additional single-cycle sine wave in the EEG with similar latency from trial to trial this might align the poststimulus phase distributions (depending on the ratio of the amplitudes of evoked to ongoing activity). However, this would be considered transient evoked activity, not the phase reset of an ongoing oscillation.

To assess the contribution of postprobe power increases to the observed phase locking, Fig. 2*d* shows the average of the power spectra for individual trials for the 1-s interval centered around probe onset. This figure shows that there is a peak in 8-Hz power both before and after the onset of the probe. However, 8-Hz power actually decreases significantly after probe onset

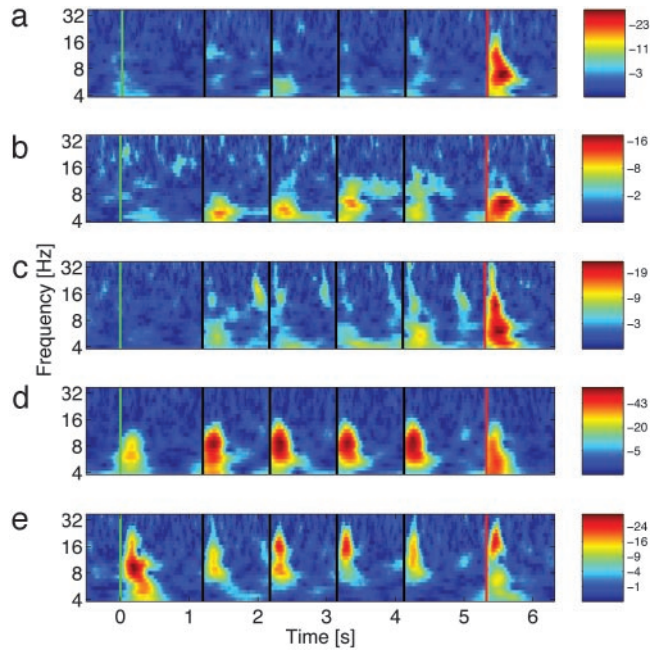


**Fig. 3.** Patterns of phase reset across brain locations. (*a*) Phase-locking spectrogram illustrating degree of phase locking across frequency and time. The color scale represents the $\log_{10}$ (*P*) value associated with the null hypothesis that the phase values (across trials) are uniformly distributed. Activity recorded from an electrode in right inferior temporal lobe in participant 9 [Talairach coordinates: (L–R, A–P, I–S) = (+14, −54, −3) mm]. Green bars denote the onset of the orienting stimulus, blue bars denote the onset of the list items, and red bars denote the onset of the probe stimulus. (*b*) Phase-locking spectrogram from an electrode in right subcallosal gyrus of participant 1 [Talairach coordinates: (L–R, A–P, I–S) = (+19, +1, −13) mm]. (*c*) Phase-locking spectrogram from a depth electrode in the right hippocampus of subject 4 [Talairach coordinates: (L-R, A-P, I-S) = (+25, −27, −19) mm]. (*d*) Phase-locking spectrogram from a depth electrode in the right occipital cortex of subject 7 [Talairach coordinates: (L–R, A–P, I–S) = (+39, −74, 3) mm]. (*e*) Phase-locking spectrogram from an electrode in the right inferior temporal lobe of subject 2 [Talairach coordinates: (L–R, A–P, I–S) = (+35, −39, −16) mm].

(df = 301, $t = 6.34$, $P < 0.01$), contradicting the hypothesis that evoked activity is contributing to the observed phase locking.

Although Fig. 2 *b* and *c* shows phase distributions of the signals from one electrode for a particular frequency and time point (250 ms before and after probe), it is of interest to comprehensively assess these effects throughout the trial and across all frequencies. Fig. 3 shows the degree of phase locking at each time point during the trial for logarithmically spaced frequencies between 4 and 55 Hz, for five different electrodes. In Fig. 3*a*, there is no discernible phase locking at any frequency after the orienting stimulus or any of the list items, but there is highly significant phase locking centered around 8 Hz after the probe. Fig. 3 *b*–*e* shows the same graph for recordings taken from four electrodes across four different participants. Fig. 3 *b* and *c* shows little or no phase locking after the orienting stimulus, a small amount of phase locking to the list items, and very strong phase locking after the probe. Fig. 3*d*, however, exhibits striking phase locking to each of the list items, less phase locking to the probe and very little phase locking to the orienting stimulus. Fig. 3*e* shows the phase-locking spectrogram for an electrode that exhibits strong phase locking to the orienting stimulus, and weaker phase locking to the list items and the probe. These figures are representative of the types of effects observed across participants and brain regions, and show that the peak of the observed phase locking typically (though not always) occurs in the 7- to 16-Hz range.

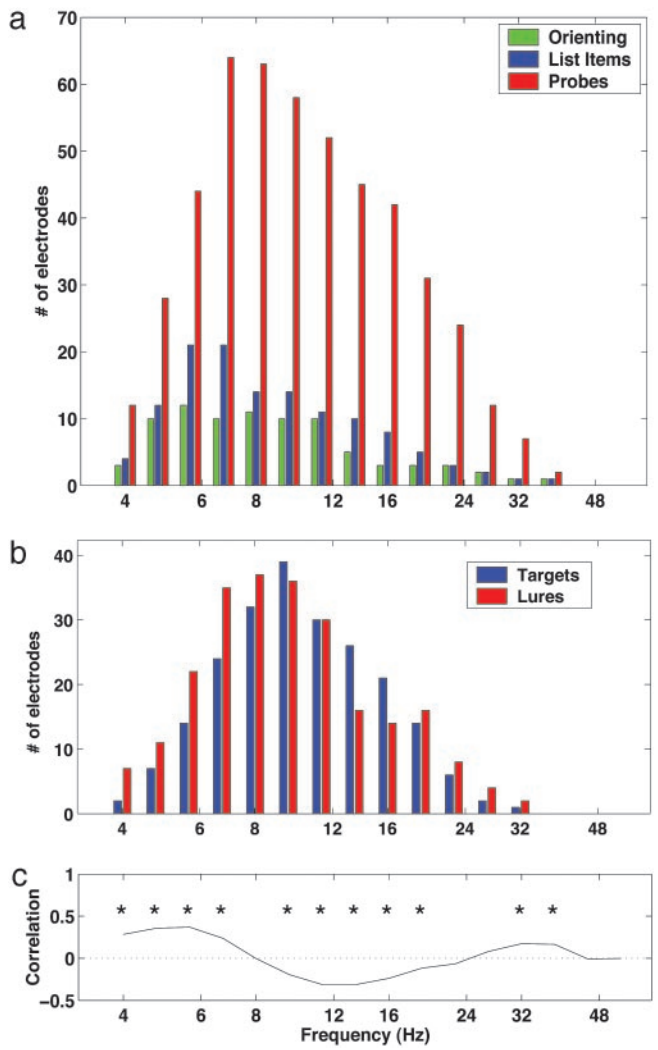


**Fig. 4.** Phase reset is neither caused by item repetition nor accompanied by transient increases in power. (*a*) Number of electrodes exhibiting significant phase reset to the orienting stimulus (green), list items (blue), and probes (red) at each frequency. (*b*) Number of electrodes exhibiting significant phase reset to targets (blue) and lures (red). Conservative estimate of Type-I error rate is less than one electrode per frequency in both panels. (*c*) Correlation between postprobe power change and phase locking at each frequency. Asterisks denote significant correlations ($P < 0.01$).

The foregoing analyses show that phase locking of oscillatory activity follows the appearance of task stimuli at specific electrodes. To examine the generality of this phenomenon we tallied the number of electrodes exhibiting significant phase locking to probes, list items, and orienting stimuli at frequencies ranging from 4 to 55 Hz. Fig. 4*a* shows widespread phase locking between 7 and 16 Hz, with many more electrodes exhibiting phase locking to probes than to study items or the orienting stimulus. Fig. 4*b* shows that comparable numbers of electrodes exhibit significant phase locking to target probes and lure probes at each frequency. The lack of any significant difference between these distributions (Kolmogorov–Smirnov test, $D = 0.08$, $P > 0.5$) suggests that the widespread phase locking to probes is not a consequence of item repetition, as only target probes are repeats of study items.

Fig. 4*c* shows the correlation (across all electrodes) between postprobe power change (paired *t* statistic) and phase locking (Rayleigh statistic) at each frequency. In the 7- to 16-Hz band, where phase locking is widespread, postprobe power correlates negatively with phase locking. The absence of significant positive

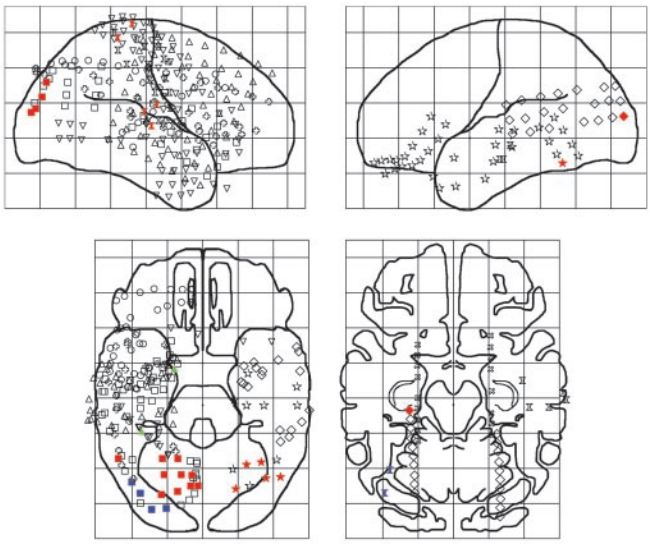

**Fig. 5.** Brain locations exhibiting preferential reset to each stimulus class. Topographic maps display the location of brain regions exhibiting preferential reset to each stimulus class. Red-, blue-, and green-filled shapes indicate preferential reset to the probe, list items, and the orienting stimulus, respectively. Unfilled shapes denote the 551 electrodes that were included in the analysis but did not exhibit preferential reset. Different shapes indicate different participants.

correlations in this band suggests that phase locking reflects reset of ongoing oscillations. However, in the 4- to 7-Hz range, where phase locking correlates positively with postprobe power changes, we cannot rule out the possibility that phase locking results from transient increases in power.

Of the 551 selected electrodes, 62 showed preferential reset at some frequency band to one of the three stimulus classes: 43 to probes, 17 to list items, and 2 to the orienting stimulus. In the 7- to 12-Hz band, where phase locking was most widespread, 27, 6, and 2 electrodes exhibited preferential reset to probes, list items, and the orienting stimulus, respectively. For each stimulus class, Table 1 gives the number of electrodes in each frequency band that exhibit preferential reset to that class. Probe-specific phase reset accounts for the greatest number of electrodes. However, list items and the orienting stimulus also elicit preferential reset in several brain locations.

Fig. 5 shows the locations of electrodes exhibiting the greatest precision of reset to each stimulus class in the 7- to 12-Hz band. The 27 electrodes exhibiting preferential reset to probes were found in the inferior temporal lobe and occipital lobes, bilaterally, as well as on the right parietal lobe. Preferential reset to list items occurred at two recording sites in the right posterior temporal lobe. Preferential reset to the orienting stimulus also appeared in two locations, both in mesial subtemporal sites in the right hemisphere. Although we also recorded from electrodes distributed across the frontal, prefrontal and suborbital frontal sites, none of these exhibited preferential reset to any stimulus class.

## Discussion

Whereas previous studies have shown that working memory demands are accompanied by increases in the amplitude of oscillations within individual brain regions (1, 10) and increased synchrony between brain regions (3), we considered whether the cognitive processes engaged by various task events might produce a reset of ongoing oscillations. Analysis of the distribution of phase across trials revealed that statistically significant phase locking followed the appearance of behaviorally relevant stimuli, including the orienting stimulus, list items, and probe. For individual electrodes, this phase locking occurred for tight clusters of frequencies (Fig. 3); however, across electrodes the effect was broadband, with a majority of sites exhibiting phase locking in the 7- to 16-Hz range (Fig. 4).

It is possible that transient, stimulus-evoked activity in the EEG causes phase locking. However, this account predicts that phase locking should be accompanied by poststimulus increases in oscillatory power. Contrary to this prediction, we observed negative or insignificantly positive correlations between phase locking and poststimulus power in the 7- to 16-Hz range, the range with the most widespread evidence for phase-locking (Fig. 4*c*). It would thus appear that phase locking at many of these sites arises from an actual reset of ongoing oscillations. Our finding of positive correlations between phase locking and power increases outside the 7- to 16-Hz range leaves open the possibility that phase locking at these frequencies arises from evoked activity.

There are several possible reasons why phase reset might be associated with decreased power, as it sometimes is. First, a reset of ongoing oscillations would produce a discontinuity in the phase of the signal. Because consistent phase is required to observe significant power, any discontinuity would reduce the measured power in the signal. Second, prestimulus power may reflect the action of multiple neural ensembles within a region sampled by a given electrode. In this case, decreased power and increased phase locking could arise if reset of oscillations within one population (activated by stimulus onset) was coupled with decreased power within a second population (inhibited by stimulus onset).

One possible role for phase reset would be to establish the synchrony between disparate brain areas that may accompany cognitive processing. A recent study by Fell *et al.* (3) suggests that gamma band phase synchrony between hippocampus and the parahippocampal region increases during successful memory encoding. A related study by Tallon-Baudry *et al.* (2) indicates that extrastriate beta-band oscillations exhibit increased phase synchrony during visual memory maintenance. Phase reset could be the mechanism by which synchrony between different brain regions is established. In fact, there is evidence from *in vitro* guinea-pig recordings suggesting that phase reset of gamma oscillations induces increased synchrony between different areas of entorhinal cortex (27).

Previous studies have tried to relate ongoing brain oscillations with the stimulus-evoked response (28–32). Analyzing scalp EEG during photic stimulation Jansen and Brandt (33) found that the prestimulus phase of alpha-band oscillations influences the latency and amplitude of the average evoked response. Tesche and Karhu (34), using magnetoencephalography, have shown that oscillatory activity to probe items increases with list length in a similar working memory task, whereas Sayers and Beagly (35) used auditory stimulation to show that, at some frequencies, poststimulus EEG phase deviates from uniformity across trials. Although both sets of authors interpreted their result as consistent with the phase reset of oscillations, in both cases their methods did not disambiguate phase reset from poststimulus increases in band power. In contrast, our results show that phase reset can be accompanied by a decrease in band power, and is not positively correlated with changes in power throughout the 7- to 16-Hz frequency band.

Makeig *et al.* (36) analyzed the relation between oscillatory phase and visual evoked potentials at the scalp. They found that 10-Hz oscillations exhibited nonrandom phase distributions after the onset of visual stimuli. Our findings of phase reset in intracranial field potentials complement their results and extend them by providing evidence that preferential reset is modulated by the behavioral demands of the task. In the 7- to 12-Hz frequency range, where phase-locking was most widespread,

recordings from 27 electrodes exhibited preferential reset to probes; recordings from only just 2 electrodes exhibited preferential reset to study items.

Phase reset also plays a role in physiologically realistic models of recognition memory. Jensen and Lisman (37) used the properties of oscillatory phase reset to fit reaction time distributions from human participants in the Sternberg task. Their model utilizes slow wave (4–12 Hz) phase reset to initiate serial scanning operations after probe onset, and is corroborated by our finding of phase reset after probe onset.

Hasselmo and colleagues (38) have proposed that the phase of hippocampal slow-wave activity is important for learning and memory. Their model utilizes weak output from hippocampal area CA3 during encoding and a strong output from CA3 during retrieval, with the phase of the oscillation playing the key role in setting the encoding/retrieval mode of the network. According to their model, slow wave phase should exhibit specific relationships to encoding and retrieval of stimuli. Specifically, encoding and retrieval operations should be 180° out of phase. The results presented here are consistent with the idea that encoding (list item) and retrieval (probe) operations have a preferred phase, and phase reset may be the method by which this preferred phase is attained during each trial.

Our observation of preferential reset to probes, list items, and the orienting stimulus (Table 1), may be a consequence of any of a number of factors that vary across stimulus classes. The appearance of the orienting stimulus alerts participants to the onset of the trial, preparing them to study the upcoming series of letters. The study phase involves two primary processes: letter identification of the list items, and encoding of the items into working memory. With the appearance of the probe, the participant is required to identify the probe, compare the probe with the stored representations of the list items, and use this comparison to drive a speeded motor response. Because letter identification should be similar during presentation of list items and probes, the preferential reset to list items (e.g., Fig. 3*e*) most likely reflects the specific demands of encoding the list items into working memory. In contrast, the preferential reset to probes, observed at the largest number of recording sites (e.g., Fig. 3 *a–d*), could reflect either the memory comparison process or motor-preparatory mechanisms. Although we cannot rule out the latter possibility, the anatomical distribution of electrodes exhibiting preferential reset to probes (Fig. 5*e*) suggests that we are not analyzing purely movement-related activity, which has been localized to the central motor areas and premotor cortex (39). Rather, it is likely that memory comparison processes, which may operate in either serial or parallel fashion (40, 21), cause preferential reset to probe items.

By directly examining phase in a task that evokes striking oscillations in human cortex, we have succeeded in demonstrating the reset of cortical oscillations. We have further shown preferential phase reset to each of the three stimulus classes in our working memory task. These results highlight the importance of phase in human neocortical oscillations and lend support to oscillatory models of memory function (37, 38).

We thank J. Lisman and our colleagues in the epilepsy programs at Children's Hospital, Brigham and Women's Hospital, and Universitaet Freiburg, including P. M. Black and B. Bourgeois. This work was supported by National Institutes of Health Grant MH55687 (to M.J.K.) and National Service Research Award MH12854 (to D.S.R.).

1. Caplan, J. B., Madsen, J. R., Raghavachari, S. & Kahana, M. J. (2001) *J. Neurosci.* **86,** 368–380.
2. Tallon-Baudry, C., Bertrand, O. & Fischer, C. (2001) *J. Neurosci.* **21,** RC177.
3. Fell, J., Klaver, P., Lehnertz, K., Grunwald, T., Schaller, C., Elger, C. E. & Fernandez, G. (2001) *Nat. Neurosci.* **4,** 1259–1264.
4. Varela, F., Lachaux, J., Rodriguez, E. & Martinerie, J. (2001) *Nat. Rev.* **2,** 229–239.
5. Kahana, M. J., Seelig, D. & Madsen, J. R. (2001) *Curr. Opin. Neurobiol.* **11,** 739–744.
6. Nunez, P. L., Srinivasan, R., Westdorp, A. F., Wijesinghe, R. S., Tucker, D. M., Silberstein, R. B. & Cadusch, P. J. (1997) *Electroencephalogr. Clin. Neurophysiol.* **103,** 499–515.
7. Sperling, M. (1997) *Epilepsia* **38,** S6–S12.
8. Fernandez, G., Effern, A., Grunwald, T., Pezer, N., Lehnertz, K., Dumplemann, M., Van Roost, D. & Elger, C. E. (1999) *Science* **285,** 1582–1585.
9. Kahana, M. J., Sekuler, R., Caplan, J. B., Kirschen, M. & Madsen, J. R. (1999) *Nature* **399,** 781–784.
10. Raghavachari, S., Kahana, M., Rizzuto, D., Caplan, J., Kirschen, M., Bourgeois, B., Madsen, J. & Lisman, J. (2001) *J. Neurosci.* **21,** 3175–3183.
11. Bland, B. H & Oddie, S. D. (2001) *Behav. Brain Res.* **127,** 119–136.
12. Buzsaki, G. (2002) *Neuron* **33,** 325–340.
13. O'Keefe, J. & Burgess, N. (1999) *Trends Cognit. Sci.* **3,** 403–406.
14. Burgess, A. & Gruzelier, J. (2000) *Psychophysiology* **37,** 596–606.
15. Huerta, P. T. & Lisman, J. E. (1993) *Nature* **364,** 723–725.
16. Pavlides, C., Greenstein, Y. J., Grudman, M. & Winson, J. (1988) *Brain Res.* **439,** 383–387.
17. Givens, B. (1996) *NeuroReport* **8,** 159–163.
18. Buzsáki, G., Grastyán, E., Tveritskaya, I. & Czopf, J. (1979) *Electroencephalogr. Clin. Neurophysiol.* **47,** 64–74.
19. Adey, W. R. & Walter, D. O. (1963) *Exp. Neurol.* **7,** 186–209.
20. Adey, W. R. (1967) in *The Neurosciences: A Study Program*, eds. Quarton, G. C., Melnechuk, T. & Schmitt, O. F. (Rockefeller Univ. Press, New York), pp. 615–633.
21. Sternberg, S. (1966) *Science* **153,** 652–654.
22. Beran, R. J. (1968) *J. App. Prob.* **5,** 177–195.
23. Beran, R. J. (1969) *Ann. Math. Statist.* **40,** 1196–1206.
24. Fisher, N. (1986) *Aust. J. Statist.* **28**, 213–219; and erratum (1986) **28,** 424.
25. Fisher, N. (1993) *Statistical Analysis of Circular Data* (Cambridge Univ. Press, Cambridge, U.K.).
26. Baddeley, A. D. & Ecob, J. R. (1973) *Q. J. Exp. Psychol.* **25,** 229–240.
27. Dickson, C. & de Curtis, M. (2002) *Hippocampus* **12,** 447–456.
28. Brandt, M. E. & Jansen, B. H. (1991) *Int. J. Neurosci.* **61,** 261–268.
29. Basar-Eroglu, C., Basar, E., Demiralp, T. & Schurmann, M. (1992) *Int. J. Psychophys.* **13,** 161–179.
30. Intriligator, J. & Polich, J. (1994) *Biol. Psychol.* **37,** 207–218.
31. Yordanova, J. & Kolev, V. (1998) *Psychophysiology* **35,** 116–126.
32. Klimesch, W., Doppelmayr, M., Schwaiger, J., Winkler, T. & Gruber, W. (2000) *Clin. Neurophys.* **111,** 781–793.
33. Jansen, B. H. & Brandt, M. E. (1991) *Electroencephalogr. Clin. Neurophysiol.* **80,** 241–250.
34. Tesche, C. D. & Karhu, J. (2000) *Proc. Nat. Acad. Sci. USA* **97,** 919–924.
35. Sayers, B. M. & Beagley, H. A. (1974) *Nature* **251,** 608–609.
36. Makeig, S., Westerfield, M., Jung, T. P., Enghoff, S., Townsend, J., Courchesne, E. & Sejnowski, T. J. (2002) *Science* **295,** 690–694.
37. Jensen, O. & Lisman, J. E. (1998) *J. Neurosci.* **18,** 10688–10699.
38. Hasselmo, M. E., Wyble, B. P. & Bodelon, C. (2002) *Neural Comp.* **14,** 793–817.
39. Praamstra, P., Stegeman, D. F., Horstink, M. W. & Cools, A. R. (1996) *Electroencephalogr. Clin. Neurophysiol.* **98,** 468–477.
40. Ratcliff, R. (1978) *Psychol. Rev.* **85,** 59–108.